Distribution of modern dinocysts in surface sediments of southern Brittany (NW France) in relation to environmental parameters: Implications for paleoreconstructions

Lambert Clément [1, *], Penaud Aurélie [2], Poirier Clément [3], Goubert Evelyne [1]

[1] Univ. Vannes (UBS), UMR 6538 Laboratoire Géosciences Océan (LGO), F-56000 Vannes, France
[2] Univ. Brest (UBO), CNRS, UMR 6538 Laboratoire Géosciences Océan (LGO), F-29280 Plouzané, France
[3] Univ. Normandie, UNICAEN, UNIROUEN, CNRS, M2C, 14000 Caen, France

* Corresponding author : Christophe Lambert, email address : clement.lambert@univ-ubs.fr

Abstract :

Dinoflagellate cyst assemblages from 15 modern surface sediment samples of the Bay of Quiberon (Southern Brittany shelf) have been examined to assess their potential as marine bio-indicators for paleoenvironmental reconstructions in a shallow coastal environment. Some discrepancies are noted in the distribution of dinocyst taxa in the study area, and particularly regarding dinocyst concentration and diversity (26 different taxa identified in total) as well as heterotrophic taxa percentages. We suggest that the proportion of heterotrophic taxa is, in an embayment of 15 m deep in average, mainly attributed to bottom water oxygenation and sediment granulometry, both acting on species-selective degradation after dinocyst deposition. More precisely, higher heterotrophic abundances are found under lower oxic conditions and in fine grain-size sediment samples, leading to caution about their use as productivity indicators in coastal environments when these parameters are not fully addressed. The comparison of the Bay of Quiberon data with surface sediment samples and top cores from previously published data makes it possible to establish a transect of the modern dinocyst distribution from inshore to offshore areas in the northern Bay of Biscay, allowing to identify different ecological groups according to the hydrological and bathymetric contexts: i) an estuarine assemblage strongly dominated by Lingulodinium machaerophorum, ii) a proximal coastal assemblage dominated by L. machaerophorum and, to a lesser extent, Spiniferites bentorii, iii) a neritic assemblage dominated by L. machaerophorum, Spiniferites ramosus and cysts of Pentapharsodinium dalei, and iv) an oceanic group dominated by Spiniferites mirabilis and Operculodinium centrocarpum.

Highlights

► Dinocyst distribution in a French coastal bay linked to environmental parameters. ► Proportions of heterotrophic dinocysts related to oxidation processes. ► Lower dinocyst diversity observed under "higher O_2-coarser sediments". ► Dinocyst distribution along a northern Bay of Biscay inshore–offshore gradient.

1. Introduction

Dinoflagellates (currently about 2,377 species known; *Gomez, 2012*) are eukaryotic unicellulars found in most aquatic environments, mainly in marine waters and in the upper part of the water column, and play an important role in the trophic network (*Dale, 1996*). Half of them are heterotrophic and feed on other dinoflagellates, microalgae, diatoms and organic debris in the water column (*Evitt, 1985; Dale, 1996*); the other half possesses chloroplasts (*Gomez, 2012*). As the vegetative growth of heterotrophic dinoflagellates is likely to be enhanced by prey availability (e.g. diatoms, autotrophic dinoflagellates, phytodetritus), they are commonly used as : i) productivity tracers in the marine realm (i.e. upwelling areas, e.g. *Radi and de Vernal, 2004; Penaud et al., 2010; Hardy et al., 2018*) as well as ii) eutrophication tracers in coastal and estuarine areas (e.g. *Dale, 1999; Matsuoka, 1999; Sangiorgi and Donders, 2004; Pospelova and Kim, 2010; Price et al., 2017, 2018; Garcìa-Moreiras et al., 2018*).

Fossilizable organic-walled dinoflagellate cysts (i.e., resting cysts corresponding to "dormant stages" mainly produced during sexual reproduction; e.g., *von Stosch, 1973*) show their highest concentrations in neritic and coastal areas (i.e. where dinoflagellate blooms can occur; *Taylor, 1987*). Organic-walled dinoflagellate cysts (dinocysts) thus represent an important group of microfossils well preserved in sediments. Previous studies carried out on modern marine sediments showed their worldwide distribution as being mainly driven by sea-surface environmental parameters such as temperature (SST for Sea-Surface Temperature), salinity (SSS for Sea-Surface Salinity), sea-ice cover duration in high latitudes, nutrient concentrations and related primary productivity regimes, as well as inshore-offshore gradients, allowing their use as powerful paleoceanographic tracers (e.g., *Dodge and Harland, 1991; Mudie et al., 2001; Marret and Zonneveld, 2003; de Vernal et al., 2013, 2020;*

Zonneveld et al., 2013; Marret et al., 2020; Van Nieuwenhove et al., 2020). However, studies on the current dinocyst diversity, concentration and distribution in coastal environments are scarce, especially for the French coasts. Along the Brittany's coasts, first steps towards understanding of the modern distribution of coastal to oceanic dinocyst taxa were initiated by *Reid (1972)*, *Morzadec-Kerfourn (1977)*, *Wall et al. (1977), Larrazabal et al. (1990),* recently complemented by *Ganne et al. (2016)* for the Loire estuary and *Lambert et al. (2017)* for the Bay of Brest. A recent spatio-temporal (i.e. in space and time) Holocene study discussed the nearshore-offshore dinocyst distribution on both sides of the freshwater front in the northern Bay of Biscay shelf (*Penaud et al., 2020*). Dinocyst species were then classified in four groups accounting for different hydrological contexts (i.e. estuarine; shallow bay to inner neritic; Iroise Sea or neritic; outer neritic to full oceanic) due to a marine (i.e. distal or offshore) to coastal (i.e. proximal or onshore) transect ranging from 2,174 m to 8 m water depth (*Penaud et al., 2020*).

In this study, we investigated 15 new surface sediment samples collected in the Bay of Quiberon (BQ), which will improve the discussion of the modern spatial dinocyst distribution in a shallow bay environment, especially focusing on rarely addressed taphonomic processes. Then, these data were compared to top cores retrieved in the southern Brittany shelf (*Naughton et al., 2007; Zumaque et al., 2017; Penaud et al., 2020*) and to surface sediments of the Loire estuary mouth (*Ganne et al., 2016*) in order to improve the understanding of the modern spatial dinocyst distribution along a macro-regional inshore-offshore transect.

2. Environmental and geographical settings of the Bay of Quiberon

The 'Mor Bras' (Fig. 1) is a bathymetric depression bordering the southern coast of Brittany. It is partially isolated from the general oceanic circulation of the Bay of Biscay and from the high energetic Atlantic swells due to a belt of shoals in the extension of the Quiberon peninsula (Fig. 1). The Bay of Quiberon (BQ), which occupies the western part of the Mor Bras, is a shallow coastal embayment (15 m depth in average) that has been submerged during the Holocene (*Baltzer et al., 2014; Menier et al., 2014*). A vast network of flooded valleys converges into the Teignouse Strait (TS on Fig. 1) which separates the Quiberon Peninsula from the Houat Island (*Vanney, 1965; Menier et al., 2014;* Fig. 1). This strait is burrowed by strong tidal currents joining the inlet of the Gulf of Morbihan and contributing to the partial isolation of the BQ from the rest of the Mor Bras by the establishment of tidal gyres (yellow arrows on Fig. 1; *Vanney, 1965; Lemoine, 1989; Tessier, 2006*).

Recent works carried out in the BQ, following high summer mortality of oysters (*Mazurié et al., 2013a, b; Stanisière et al., 2013*), have shown that the shallower parts of the BQ (between 0 and 6 m deep) are mainly composed of sandy sediments, due to strong wind-forced water column mixing, while the deepest parts of the BQ are covered with muddy sediments. This sediment distribution is associated with a heterogeneous distribution of benthic foraminiferal species, analyzed in the framework of the RISCO project ('*Comité régional de la conchyliculture Bretagne Sud*' and Ifremer; 2010-2013; coord. J. Mazurié; *Mazurié et al., 2013a, b; Stanisière et al., 2013*). Among the high foraminiferal diversity studied, some taxa are characteristic of the deepest and fine grain-sized BQ areas (i.e. *Cribroelphidium gerthi, Elphidium earlandi, Gavelinopsis nitida, Lagena sulcata, Lagena semistriata, Lamarckina haliotidea, Planorbulina mediterranensis, Trifarina angulosa,* and *Textularia truncata*). They form the 'deepest foraminiferal assemblage', noted 'DeepForam' hereafter.

3. Methods

3.1. Sampling and environmental parameters

3.1.1. Data collection

The sampling campaign was carried out in 2010 in the framework of the RISCO project in 15 sites within the BQ using a 50 x 50 cm Van Veen grab for the optimal preservation of surface sediments (*Mazurié et al., 2013a, b; Stanisère et al., 2013*; Fig. 1). The first cm of each site was sampled (Table 1) for grain-size and microfossil analyses. All samples were stored in sealed vials with ethanol.

For grain-size analyses, sediments were passed through a column of sieves with different sizes of apertures (i.e. 2 mm, 500 µm, 125 µm and 45 µm). Averaged percentages of the fine sediment fraction (i.e. <125 µm, referred to as 'granulo<125' hereafter; Table 2) were considered in this study (*Mazurié et al., 2013a, b; Stanisère et al., 2013)*.

In addition, we compiled the monthly measurements of the bottom water physico-chemical parameters measured at each station to obtain averaged values for the year 2010 (Table 2). Bottom water temperature (referred to as 'Temp' hereafter), bottom water salinity ('Sal'), dissolved oxygen concentration in bottom waters ('O2'), bottom water turbidity ('Turb') and Chlorophyll a concentration in bottom water ('Chla') were measured with an MP6 probe (NKE). In addition, bottom water samples were taken from each station to calculate the suspended matter concentration ('SM') using vacuum pump filtration. Annual averaged values will be considered in this study (Table 2).

3.1.2. Correlation matrix of variables

A correlation matrix of variables was performed with the "Analysis Toolpack" of Microsoft Excel 2016, to assess the relationship between: i) sedimentological ('granulo<125', subsection 3.1.1) and foraminiferal ('DeepForam', section 2) data, ii) dinocyst data ('Cdino', subsection 3.2.1.; and 'Srdino', 'Hdino', subsection 3.2.2.) and iii) the measured environmental variables ('Depth', 'Temp', 'Sal', 'O2', 'Chla', 'Turb', 'SM', subsection 3.1.1).

The matrix consists of Pearson correlation coefficients (r) between each variable that range from -1 to 1. If r=0, no linear correlation exists between compared variables. The greater the absolute value of r, the stronger the correlation: positive when approaching 1 and negative when approaching -1. Statistical significance is expressed by the p-value. P-value < 0.05 indicates a strong presumption against the null hypothesis and a good confidence in the statistical correlation expressed by the Pearson coefficients.

3.2. Dinoflagellate cyst analysis

3.2.1. Laboratory procedure for palynological slides

Dinocyst extraction was performed at the UMR 6538 CNRS (LGO-*Laboratoire Géosciences Océan*, UBO-University of Brest) from the 10–150 μm sediment fraction. Three cm^3 of fifteen BQ surface sediment samples (samples from December 2010) were analyzed following a standard protocol described by *de Vernal et al. (1999)* that includes 10% cold HCl and 70% cold HF to remove carbonate and siliceous fractions, respectively. The final residues were mounted between slides and coverslips with glycerol. Dinocyst concentrations ('Cdino'; Table 2), expressed in number of cysts per cm^3 of dry sediments (cysts/cm^3) were calculated thanks to the marker grain method (*Stockmarr, 1971; de Vernal et al., 1999*; *Mertens et al., 2009*). This method consists in adding aliquot volumes of *Lycopodium* spores before the

palynological treatment, these exotic spores being counted in parallel with fossilized palynomorphs.

3.2.2 Dinocyst identification, diversity indexes and statistical analysis

For each analyzed sample, except BQ sample n°3 (cf. Fig. 1), a minimum of 150 dinocysts was reached, using an Olympus CH-2 optical microscope (at magnifications ×630 and ×1000), in order to provide robust assemblages from a statistical point of view. The threshold of 100 individuals is indeed required to identify 99% of major (>5%) species (*Fatela and Taborda, 2002*) and thus robust to discuss the proportion of the two large groups of dinocysts (i.e. the strict heterotrophic taxa vs. the other dinocysts). The BQ sample n°3, mainly characterized by coarse sediments (i.e. 63% of grain sizes exceed 125μm), must be interpreted with caution since only 13 specimens were counted. Taxa identification followed *Rochon et al. (1999)*, *Zonneveld & Pospelova (2015)* and *Van Nieuwenhove et al. (2020)*. Dinocyst percentages were calculated for each taxon (list of identified taxa in Table 3), on a main sum including all taxa and excluding non-identified ones (always less than three undetermined specimens per analyzed level).

We use the Shannon Diversity index to estimate the dinocyst diversity as an additional ecological indicator (noted 'Srdino' hereafter for Species Richness; Table 2). The Shannon index provides information both on specific richness and on the structure of populations. The higher the value, the greater the taxa diversity and the more homogeneous the relative abundances. In addition, we calculated the total percentages of brown cysts from heterotrophic dinoflagellates, or heterotrophic dinocysts ('Hdino'; Table 2). Cluster analysis was also conducted on the 15 samples, using PAST v.1.75b (*Hammer et al., 2001*), according

to dinocyst assemblages to better highlight similarities and differences between analyzed samples.

3.2.3 Inshore-offshore transect

In order to discuss dinocyst diversity changes along an inshore-offshore gradient on a larger-scale, we also compared dinocyst assemblages from surface sediments and core tops taken in the northern Bay of Biscay, in different environmental and bathymetric contexts: i) two samples taken in the downstream Loire Estuary (*Ganne et al., 2016*) are representative of the Loire river mouth, ii) the averaged 15 surface samples of this study account for the shallow coastal BQ, iii) a sample from the top core section (level 47 cm) of the CBT-CS11 core (73 m water depth) is representative of the shelf under mixed oceanic and winter fluvial influences (*Penaud et al., 2020*), iv) a sample from top core section (level 4 cm) of the VK03-58bis core (97 m water depth) is representative of the deeper shelf (*Naughton et al., 2007*). Regarding these last two sites, we targeted the two "modern" samples on the basis of palynological evidence unambiguously signaling for their contemporaneity (i.e., presence of pollen grains of *Zea mays*). The distal MD95-2002 core, taken off the Armorican margin at 2,200 m deep, has finally been added to the transect (*Zumaque et al., 2017*). The top core sample (0 cm) is estimated at ca. 1,000 Cal. years BP and is therefore representative of late Holocene conditions (*Zumaque et al., 2017*). Such a gradient in dinocyst distribution as a function of the distance to the coast therefore provides a baseline reference for inferring dinocyst-derived past environmental changes on the temperate north-eastern Atlantic margin.

4. Results

4.1. Cluster analysis between study samples

All studied stations are represented within the BQ with a colour code corresponding to the result of the cluster analysis (Figs. 2a, b).

Station n°3 stands out from the others with a low similarity coefficient (i.e. around 0.65; Fig. 2a). The coarse grain size (Fig. 2h) and the related very low dinocyst concentration (Figs. 2c and 3a) characterizing this station set it apart from the others. With the exception of station n°5, all stations located below the 6 m isobath (n°2, 10, 15, 11, 13, 12, 8, and 14) are grouped together in a same cluster (brown colour, Figs. 2a,b) with a high coefficient of similarity (> 0.825; Fig. 2a), and stations located above the 6 m bathymetric threshold (n°4, 6, and 9) are grouped in a same cluster (green colour, Figs. 2a,b) with the additional sites n°7 and 1. All these shallowest sites are characterized by generally coarser grain-size values (Fig. 2h).

4.2. Dinoflagellate cyst results

Dinocyst concentrations of the 15 surface sediment samples range from ca. 300 to 18,300 cysts/cm^3 with a mean of ca. 8,100 cysts/cm^3 (standard deviation of ca. 5,300 cysts/cm^3) (Fig. 3a). The lowest values correspond to the shallowest sites located to the north and west of the BQ whereas the highest ones are recorded at the deepest sites, below the 6 m isobath (Figs. 2c and 3a).

A total of 26 different dinocyst taxa was identified (12 autotrophic and 14 heterotrophic taxa; cf. Table 3) with an average of 14 different taxa per sample (Fig. 3a). Assemblages (Figs. 3a,b) are largely dominated by *Lingulodinium machaerophorum* (45 % in average; Fig. 3b), commonly found dominant in areas with strong fluvial influences (*Morzadec-Kerfourne,*

1977; Ganne et al., 2016; Lambert et al., 2017; Penaud et al., 2020). The other major autotrophic taxa are *Spiniferites bentorii* (11 % in average; Fig. 3b), *Spiniferites membranaceus* (6 % in average; Fig. 3b) and cysts of *Pentapharsodinium dalei* (5 % in average; Fig. 3b).

The heterotrophic rate is on average 20 % over the whole BQ (Fig. 3b) and is particularly represented by *Brigantedinium* spp. species (i.e. "round brown" cysts produced by *Protoperidinium* dinoflagellate species) (12 % in average; Fig. 3b). The highest relative abundances of heterotrophic cysts (Figs. 2e, 3a) are generally observed in the deepest areas of the BQ (Fig. 2), between 6 and 10 m, which are characterized by the lowest bottom water oxygen concentrations (Fig. 2g) and the lowest sediment grain-size values (Fig. 2h). The total dinocyst concentrations (Figs. 2c, 3a) and in a lesser extent the specific richness (Fig. 2d) follow the same trend. The 6 m isobath therefore seems to constitute a limit below which dinocyst concentrations are greater.

4.3. Correlation matrix of variables

The correlation matrix of variables (Fig. 4) shows strong correlations between the different variables here used to explain the dinocyst distribution. Among these, a ~~good~~ positive correlation ($r > 0.5$) is noted between 'Hdino' and three variables: 'depth', 'granulo<125' and 'DeepForam' (Fig. 4). Heterotrophic dinocysts therefore increase with the bathymetry, in parallel with finer sediments and increasing occurrences of the deepest foraminiferal taxa. Also, a similar correlation with 'depth', 'granulo<125' and 'DeepForam' is observed with 'Cdino' and 'Srdino' (Fig. 4), likely caused by the greater occurrences of heterotrophics in the deepest zones of the BQ (> 6 m). Finally, a good positive correlation is noted between

'Srdino', 'Cdino', and to a lesser extent 'Hdino', and on the other hand 'O2', while 'Hdino' is little or not correlated with "Chla" (Fig. 4).

5. Discussion

5.1. Taphonomic issues and dinocyst preservation in the Bay of Quiberon

Some discrepancies in dinocyst distribution are observed within the BQ, especially for the heterotrophic taxa, showing slightly higher occurrences in the deepest areas (below the 6 m bathymetric threshold; Figs. 2e and 3a; Fig. 4). Furthermore, we assume that the small BQ (i.e. 40 km²), characterized by strong tidal currents (cf. gyratory circulation in Fig. 1) which homogenize surface water properties including nutrients (*Tessier, 2006*), cannot explain the differential distribution of heterotrophic dinocysts in the BQ (Figs. 2e and 3a). *Brigantedinium* species, which dominate the heterotrophic assemblages (Fig. 3), as well as *Echinidinium* species, are sensitive to oxidation (*Zonneveld et al., 1997; Kodrans-Nsiah et al., 2008; Bogus et al., 2014*). Their occurrences even decrease logarithmically with increasing bottom water oxygen concentrations (*Zonneveld et al., 2001, 2007, 2008*). Double-walled organic dinocysts (i.e. dormant resting stages with a mandatory dormancy period; *Anderson and Wall, 1978*) are composed of a macromolecule, whose chemical composition consists in a cellulose-like glucan in autotrophic, and a nitrogen-rich glycan in heterotrophic forms (*Bogus et al.,2014*). This difference in dinocyst chemical composition explains the greater vulnerability of heterotrophics to oxidation and a differential preservation during diagenetic processes (*Bogus et al., 2014*).

In our study, statistical correlation between the percentages of heterotrophic dinocysts and measured environmental parameters allowed us to discuss the significance of the heterotrophic signature in the BQ (Fig. 4). A lack of correlation between 'Chla' and 'Hdino' (r = -0.06; Fig. 4) suggests that productivity is not a main factor explaining differences in the

BQ spatial distribution of heterotrophic dinocysts. The weak negative correlation observed between heterotrophic cysts ('Hdino') and 'O2' (r = -0.25; Fig. 4) is mitigated by a non-obvious statistical correlation (p-value=0.369; Fig. 4). Moreover, dissolved oxygen values ('O2'), are derived from occasional measurements and are not representative of an averaged state of the BQ bottom water oxygenation. Indeed, seasonal hypoxia have been recognized in the deepest areas of the BQ and related to the establishment of a seasonal water column stratification, with oyster mortality below the bathymetric threshold of 6 m (*Stanisière et al., 2013*). Therefore, to test the effect of heterotrophic degradation(/preservation) under oxic(/anoxic) conditions, benthic foraminiferal data have been additionally considered. The deepest benthic foraminiferal assemblage considered ('DeepForam'; Fig. 2f) is mainly constituted by opportunistic species and characterize areas subjected to seasonal hypoxia, confirming the modern environmental assessment (*Stanisière at al., 2013*). It is also worth noting that the water column stratification and its effects on the seasonal bottom water oxygen depletion from the 6 m isobath, is also confirmed by i) the negative correlation between 'depth' and 'Temp' (r = -0.79; Fig. 4), as well as between 'depth' and 'O$_2$' (r = -0.70; Fig. 4), and ii) the positive correlation between 'depth' and 'DeepForam' (r = 0.95; Fig. 4). The positive correlations we observed between 'DeepForam' and 'Hdino' (r = 0.76; Fig. 4), 'DeepForam' and 'Srdino' (r = 0.49; Fig. 4) and 'DeepForam' and 'Cdino' (r = 0.57; Fig. 4) therefore suggest that depleted oxygen concentrations may be involved in the higher dinocyst preservation by increasing heterotrophic taxa percentages and dinocyst concentrations. The heterotrophic signature also seems to be correlated with grain-size values. The distribution map (Fig. 2h) and the Pearson correlation coefficient (Fig. 4) show that the proportion of the finest sediments increases with depth. A significant correlation is highlighted between 'granulo<125' and 'Hdino' (r = 0.56; Fig. 4), 'granulo<125' and 'Srdino' (r = 0.61; Fig. 4) and 'granulo<125' and 'Cdino' (r = 0.75; Fig. 4). It is well-known that coarser sediments are

not conducive to a good preservation of palynomorphs (cf. example of sampling site n°3 in the BQ; Fig. 3a) due to interstitial fluid circulation and higher oxygenation in a porous sediment. The coarser the sediment, the lower the proportion of heterotrophics (Figs. 2e, h). Variations in the proportions of heterotrophics may thus be related to the effect of oxidation processes acting on species-selective degradation after cyst deposition in the BQ.

A conceptual model allows gathering environmental conditions prevailing in the BQ to explain the differential dinocyst distribution pattern (Fig. 5). At the scale of the study area, we postulate that "autotrophic/heterotrophic" dinocyst fluxes to the sediments are almost identical at all points of the BQ (red arrows on Fig. 5), due to a bay-wide homogenization of sea-surface properties through tidal currents. Beyond 6 m deep, the water column stratification results in an oxygen bottom-water consumption which exceeds its renewal and thus in seasonal bottom-water hypoxia. Because of this stratification, the weakening of coastal and tidal currents in the deepest areas of the BQ enhanced the sedimentation of finer sediments. The combination of seasonal bottom-water oxygen depletion and higher proportion of finer sediments may explain the greater occurrences of heterotrophics below the 6 m isobath.

Such considerations lead us to consider with great caution, in shallow-bay paleoecological reconstructions, the use of heterotrophic-derived productivity indexes. In this context, *Zonneveld et al. (2007)* suggested the use of the absolute concentrations of autotrophic dinocysts rather than total or heterotrophic concentrations to discuss varying productivity conditions. Also, since the sediment granulometry plays a crucial role in the dinocyst preservation, it appears essential to carry out grain-size analyses along core or to work in homogeneous sediment contexts.

5.2. Inshore-Offshore dinocyst assemblages across the Southern Brittany shelf

The influence of environmental parameters on the dinocyst distribution is increasingly understood thanks to the gradual improvement of the world marine current databases and atlases (*e.g. Zonneveld et al., 2013; Marret et al., 2020; de Vernal et al., 2020; Van Nieuwenhove et al., 2020*). However, although the highest dinocyst concentrations are observed in neritic and coastal areas, studies on current dinocyst distributions in French coastal environments are still scarce (e.g. *Morzadec-Kerfourn, 1977; Larrazabal et al., 1990; Ganne et al., 2016; Lambert et al., 2017*). From previous studies (*e.g. Williams, 1971; Morzadec-Kerfourn, 1977; Penaud et al., 2020*), dinocyst groups have been established: i) the oceanic zone (>100-150 m water depth, outer-neritic assemblage) appears characterized by *Impagidinium aculeatum, O. centrocarpum, S. mirabilis*, and *S. elongatus* (with *S. ramosus* and *S. bulloideus* in addition), *I. aculeatum* being restricted to full-oceanic waters, ii) the coastal zone (inner-neritic) is characterized by the association *S. ramosus-S. bulloideus-S. bentorii*, and iii) the estuarine coastal zone, under fluvial-derived major influence, is characterized by *L. machaerophorum*, a species tolerant to large drops in salinity and mainly proliferating in brackish environments (*Reid, 1975; Morzadec-Kerfourn, 1977, 1997; Mudie et al., 2017; Penaud et al., 2020*).

Along the inshore-offshore gradient (Fig. 6a), estuarine to inner-neritic samples under strong fluvial influences exhibit an almost monospecific assemblage of *L. machaerophorum* (more than 80 %; Fig. 6b). *L. machaerophorum* is becoming less and less abundant with the distance from the coast and is rarely observed in the full-oceanic environment (i.e. around 0.3% in the MD95-2002 core; Fig. 6b). The offshore sea-surface conditions are indeed influenced by the North Atlantic general circulation, while the circulation on the continental shelf is influenced

by a mixed river / tidal current limited to the coast (*Penaud et al., 2020*). In shelf sediments (CBT-CS11 and VK03-58bis cores), the prevalence of the *L. machaerophorum* species over neritic to oceanic cyst taxa thus suggests seasonally coastal stratified waters subjected to strong continental influence (*Penaud et al., 2020*). Indeed, from mid-autumn to early spring, strong river flows (*i.e.* Gironde, Loire, Vilaine) associated with sustained northeastward wind activity maintain this region under the influence of northward freshwater plumes and associated low salinities between the coast and the 100 m isobath (*Lazure et al., 2008; Charria et al., 2013; Costoya et al., 2015, 2016*). The resulting density gradients explain water mass stratification and thermohaline front at the 100 m isobath, and thus the prevalence of *L. machaerophorum* until this limit *(Penaud et al., 2020)*.

The transect confirms the ecological preferences of *S. bentorii* and *S. ramosus* for the coastal environments. However, while *S. bentorii* seems to be a good marker of the strict proximal domain (i.e. strong occurrence in BQ: 11.7 %; Fig. 6b), being almost absent from the shelf (i.e. VK03-58bis and CBT-CS11 cores: 0.3 and 2 %, respectively), *S. ramosus* exhibits an inverse distribution and becomes more and more present away from the coast (Fig. 6b): *S. ramosus* reaches 5% in the full-oceanic domain (MD95-2002 core) while *S. bentorii* is totally absent. *S. ramosus* and *S. bentorii* can therefore be considered as excellent markers of the proximal neritic environment under moderate fluvial influences. Cysts of *P. dalei* show a fairly homogeneous distribution and low percentages all along the transect (i.e. 3 to 10%; Fig. 6b), being more dominant in northern latitudes of the North Atlantic Ocean and in fjords (*Mudie and Rochon, 2001; Zonneveld et al., 2013; Heikkilä et al., 2014; Marret et al., 2020*). This species also occurs in environments where upper water salinities are reduced as a result of meltwater or river inputs (*Zonneveld et al., 2013*). The neritic zone of the southern Brittany shelf, marked by a winter salinity front, may explain its greater occurrence in the proximal zone of the continental shelf (*i.e.* CBT-CS11 and BQ; 12 % and 5 %, respectively). In

temperate waters, cysts of *P. dalei* may likely be used as indicators of cooling and/or continental influences. *S. mirabilis* and *O. centrocarpum* are not significant in the Loire Estuary and in the other three coastal sites (i.e. BQ, CBT-CS11 and VK03-58bis; Fig. 6b), whereas both taxa respectively reach 53 and 21% in the deepest site (i.e. MD95-2002; Fig. 6b). These results confirm their affinity for full-oceanic North Atlantic areas. The distribution of heterotrophic dinocysts along this transect is more difficult to interpret. Although we cannot exclude an influence of productivity conditions on heterotrophics, their virtual absence from the Loire Estuary (LE; Fig. 6b) raises questions as it is the most productive area of the transect (*Gohin et al., 2019*). As previously mentioned in section 5.1, conditions of oxygenation may result in differences between heterotrophic preservation. Comparing heterotrophics would also require to consider mean bottom oxygen conditions and grain-size values for each analyzed site.

6. Conclusion

The Bay of Quiberon (BQ), characterized by seasonal hypoxia, appears appropriate to investigate the effects of the different degrees of bottom water oxygenation on dinocyst taphonomic processes (i.e. species-selective degradation after cyst deposition). Among dinocyst assemblages, heterotrophic taxa, well-known to be sensitive to degradation processes, here show a spatial distribution that appears mainly controlled by bottom-water oxygen conditions and sediment granulometry; lower heterotrophic percentages and dinocyst diversity are observed under "higher O_2-coarser sediments". Heterotrophic occurrences in coastal sediments are here mainly associated to oxidation processes, leading to caution about their use as productivity indexes in paleoecological reconstructions carried out in these kinds

of shallow environments, unless high-resolution grain-size analyses are at least conducted in parallel with palynological studies to avoid misinterpretations.

The comparison of the averaged dinocyst results acquired in the BQ with surface sediments and top cores, issued from already published data, made it possible to improve our knowledge regarding the dinocyst distribution along a northern Bay of Biscay (southern Brittany) inshore-offshore gradient. We highlighted clear different ecological groups according to the hydrological and bathymetric contexts: i) an estuarine assemblage at the outlet of the Loire river strongly dominated by *L. machaerophorum*, ii) a proximal coastal assemblage in the shallow BQ still dominated by *L. machaerophorum* with, to a lesser extent, *S. bentorii* and *S. membranaceus*, iii) a neritic assemblage dominated by *L. machaerophorum*, *S. ramosus* and cysts of *P. dalei*, and iv) an oceanic group dominated by *S. mirabilis* and *O. centrocarpum* and in which *L. machaerophorum* is rare or absent.

7. Acknowledgment

8. Data availability

The dinocyst dataset related to this article (dinocyst counts on the 15 samples collected in the Bay of Quiberon) can be found in the supplementary material.

9. Declaration of competing interest

The authors declare that they have no competing interests.

10. References

Baltzer, A., Walter-Simonnet, A. V., Mokeddem, Z., Tessier, B., Goubert, E., Cassen, S., Diffo, A., 2014. Climatically-driven impacts on sedimentation processes in the Bay of Quiberon (south Brittany, France) over the last 10,000 years. The Holocene, 24(6), 679-688.

Bogus, K., Mertens, K. N., Lauwaert, J., Harding, I. C., Vrielinck, H., Zonneveld, K. A., Versteegh, G. J., 2014. Differences in the chemical composition of organic-walled dinoflagellate resting cysts from phototrophic and heterotrophic dinoflagellates. Journal of Phycology, 50(2), 254-266.

Charria, G., Lazure, P., Le Cann, B., Serpette, A., Reverdin, G., Louazel, S., Batifoulier, F., Dumas, F., Pichon, A., Morel, Y., 2013. Surface layer circulation derived from Lagrangian drifters in the Bay of Biscay. Journal of Marine Systems, 109, S60-S76.

Costoya, X., Decastro, M., Gómez-Gesteira, M., Santos, F., 2015. Changes in sea surface temperature seasonality in the Bay of Biscay over the last decades (1982–2014). Journal of Marine Systems, 150, 91-101.

Costoya, X., Fernández-Nóvoa, D., Decastro, M., Santos, F., Lazure, P., Gómez-Gesteira, M., 2016. Modulation of sea surface temperature warming in the Bay of Biscay by Loire and Gironde Rivers. Journal of Geophysical Research: Oceans, 121(1), 966-979.

Dale, B., 1996. Dinoflagellate cyst ecology: modeling and geological applications. In: Jansonius, J., McGregor, D.C. (Eds.), Palynology: Principles and Applications. American Association of Stratigraphic Palynologists Foundation, Dallas, pp. 1249–1276.

Dale, B., Thorsen, T. A., Fjellsa, A., 1999. Dinoflagellate cysts as indicators of cultural eutrophication in the Oslofjord, Norway. Estuarine, Coastal and Shelf Science, 48(3), 371-382.

de Vernal, A., Henry, M., Bilodeau, G., 1999. Techniques de préparation et d'analyse en micropaléontologie. Les cahiers du GEOTOP, 3, 41.

de Vernal, A., Hillaire-Marcel, C., Rochon, A., Fréchette, B., Henry, M., Solignac, S., Bonnet, S., 2013. Dinocyst-based reconstructions of sea ice cover concentration during the Holocene in the Arctic Ocean, the northern North Atlantic Ocean and its adjacent seas. Quaternary Science Reviews, 79, 111-121.

de Vernal, A., Radi, T., Zaragosi, S., Van Nieuwenhove, N., Rochon, A., Allan, E., De Schepper, S., Eynaud, F., Head, M. J., Limoges, A., Londeix, L., Marret, F., Matthiessen, J., Penaud, A., Pospelova, V., Price, A., Richerol, T., 2020. Distribution of common modern dinoflagellate cyst taxa in surface sediments of the Northern Hemisphere in relation to environmental parameters: The new n= 1968 database. Marine Micropaleontology, 159, 101796.

Dodge, J. D., Harland, R., 1991. The distribution of planktonic dinoflagellates and their cysts in the eastern and northeastern Atlantic Ocean. New Phytologist, 118(4), 593-603.

Evitt, W. R., 1985. Sporopollenin Dinoflagellate Cysts: Their Morphology and Interpretation. American Association of Stratigraphic Palynologists Foundation, Austin, Te. USA.

Fatela, F., Taborda, R., 2002. Confidence limits of species proportions in microfossil assemblages. Marine Micropaleontology, 45(2), 169-174.

Ganne, A., Leroyer, C., Penaud, A., Mojtahid, M., 2016. Present-day palynomorph deposits in an estuarine context: The case of the Loire Estuary. Journal of Sea Research, 118, 35-51.

García-Moreiras, I., Pospelova, V., García-Gil, S., Sobrino, C. M., 2018. Climatic and anthropogenic impacts on the Ría de Vigo (NW Iberia) over the last two centuries: A high-resolution dinoflagellate cyst sedimentary record. Palaeogeography, Palaeoclimatology, Palaeoecology, 504, 201-218.

Gohin, F., Van der Zande, D., Tilstone, G., Eleveld, M. A., Lefebvre, A., Andrieux-Loyer, F., Blauw, A. N., Bryère, P., Devreker, D., Garnesson, P., Hernandez Fariñas, T., Lamaury, Y., Lampert, L., Lavigne, H., Menet-Nedelec, F., Pardo, S., Saulquin, B., 2019. Twenty years of satellite and in situ observations of surface chlorophyll-a from the northern Bay of Biscay to the eastern English Channel. Is the water quality improving?. Remote Sensing of Environment, 233, 111343.

Gómez, F., 2012. A quantitative review of the lifestyle, habitat and trophic diversity of dinoflagellates (Dinoflagellata, Alveolata). Systematics and Biodiversity, 10(3), 267-275

Hallegraeff, G. M., 1995. Harmful algal blooms: a global overview, p. 1–22. In G. M. Hallegraeff, D. M. Anderson, and A. D. Cembella (ed.), Manual on harmful marine microalgae. UNESCO, Paris, France.

Hammer, Ø., Harper, D. A., Ryan, P. D., 2001. PAST: Paleontological statistics software package for education and data analysis. Palaeontologia electronica, 4(1), 9.

Hardy, W., Marret, F., Penaud, A., Le Mezo, P., Droz, L., Marsset, T., Kageyama, M., 2018. Quantification of last glacial-Holocene net primary productivity and upwelling activity in the equatorial eastern Atlantic with a revised modern dinocyst database. Palaeogeography, Palaeoclimatology, Palaeoecology, 505, 410-427.

Heikkilä, M., Pospelova, V., Hochheim, K. P., Kuzyk, Z. Z. A., Stern, G. A., Barber, D. G., Macdonald, R. W., 2014. Surface sediment dinoflagellate cysts from the Hudson Bay system and their relation to freshwater and nutrient cycling. Marine Micropaleontology, 106, 79-109.

Kodrans-Nsiah, M., de Lange, G. J., Zonneveld, K. A., 2008. A natural exposure experiment on short-term species-selective aerobic degradation of dinoflagellate cysts. Review of Palaeobotany and Palynology, 152(1-2), 32-39.

Lambert, C., Vidal, M., Penaud, A., Combourieu-Nebout, N., Lebreton, V., Ragueneau, O., Gregoire, G., 2017. Modern palynological record in the Bay of Brest (NW France): Signal calibration for palaeo-reconstructions. Review of Palaeobotany and Palynology, 244, 13-25.

Larrazabal, M. E., Lassus, P., Maggi, P., Bardouil, M., 1990. Kystes modernes de dinoflagellés en baie de Vilaine-Bretagne sud (France). Cryptogamie, Algologie, 11(3), 171-185.

Lassus, P., Chomerat, N., Hess, P., Nezan, E., 2016. Toxic and Harmful Microalgae of the World Ocean. IOC Manuals and Guides, 68.

Lazure, P., Dumas, F., Vrignaud, C., 2008. Circulation on the Armorican shelf (Bay of Biscay) in autumn. Journal of Marine systems, 72(1-4), 218-237.

Lemoine, G., 1989. Étude sédimentaire de la Baie de Quiberon : la zone ostréicole en eau profonde et ses abords. Rapport de stage. https://archimer.ifremer.fr/doc/00000/2210/

Marret, F., Zonneveld, K. A., 2003. Atlas of modern organic-walled dinoflagellate cyst distribution. Review of Palaeobotany and Palynology, 125(1-2), 1-200.

Marret, F., Bradley, L., de Vernal, A., Hardy, W., Kim, S. Y., Mudie, P., Penaud, A., Pospelova, V., Price, A. M., Radi, T., Rochon, A., 2020. From bi-polar to regional distribution of modern dinoflagellate cysts, an overview of their biogeography. Marine Micropaleontology, 159, 101753.

Matsuoka, K., 1999. Eutrophication process recorded in dinoflagellate cyst assemblages - a case of Yokohama Port, Tokyo Bay, Japan. Science of the Total Environment, 231(1), 17-35.

Mazurié, J., Stanisiere, J. Y., Langlade, A., Bouget, J. F., Dumas, F., Treguier, C., Leclerc, E., Ravaud, E., Quinsat, K., Gabellec, R., Retho, M., Cochet, H., Dreano, A., 2013b. *Les risques conchylicoles en Baie de Quiberon. Première partie : le risque de mortalité virale du naissain d'huître creuse Crassostra gigas*. Rapport final du projet Risco 2010-2013. RST/LER/MPL/13.19.

Mazurié, J., Stanisiere, J. Y., Bouget, J. F., Langlade, A., Leclerc, E., Quinsat, K., Herve, G., Augustin, J. M., Ehrhold, A., Sinquin, J. M., Meidi-Deviarni, I., Goubert, E., Cochet, H.,

Dreano, A., 2013b. *Les risques conchylicoles en Baie de Quiberon. Deuxième partie : le risque de prédation sur l'huître creuse <u>Crassostrea gigas</u>.* Rapport final du projet Risco 2010-2013. RST/LER/MPL/13-20.

Menier, D., Augris, C., Briend, C., 2014. *Les réseaux fluviatiles anciens du plateau continental de Bretagne Sud.* Editions Quae, p 104.

Mertens, K. N., Verhoeven, K., Verleye, T., Louwye, S., Amorim, A., Ribeiro, S., Deaf, A. S., Harding, I. C., De Schepper, S., Gonzalez, C., Kodrans-Nsiah, M., de Vernal, A., Henry, M., Radi, T., Dybkjaer, K., Poulsen, N. E., Feist-Burkhardt, S., Chitolie, J., Heilmann-Clausen, C., Londeix, L., Turon, J. L., Marret, F. Matthiessen, J., McCarthy, F. M. G., Prasad, V., Pospelova, V., Kyffin Hughes, J. F. Riding, J. B., Rochon, A., Sangiorgi, F., Welters, N., Sinclair, N., Thun, C., Soliman, A. Van Nieuwenhove, N., Vink, A., Young, M., 2009. Determining the absolute abundance of dinoflagellate cysts in recent marine sediments: the Lycopodium marker-grain method put to the test. Review of Palaeobotany and Palynology, 157(3-4), 238-252.

Morzadec-Kerfourn, M. T., 1977. Les Kystes de dinoflagellés dans les sédiments récents le long des côtes Bretonnes. Revue de Micropaléontologie, 20, 157-66.

Morzadec-Kerfourn, M. T., 1997. Dinoflagellate cysts and the paleoenvironment of Late-Pliocene early-pleistocene deposits of Brittany, Northwest France. Quaternary Science Reviews, 16(8), 883-898.

Mudie, P.J., Harland, R., Matthiessen, J., de Vernal, A., 2001. Dinoflagellate cysts and high latitude Quaternary paleoenvironmental reconstructions: an introduction. Journal of Quaternary Science, 16, 595–602.

Mudie, P. J., Rochon, A., 2001. Distribution of dinoflagellate cysts in the Canadian Arctic marine region. Journal of Quaternary Science: Published for the Quaternary Research Association, 16(7), 603-620.

Mudie, P. J., Marret, F., Mertens, K. N., Shumilovskikh, L., Leroy, S. A, 2017. Atlas of modern dinoflagellate cyst distributions in the Black Sea Corridor: from Aegean to Aral Seas, including Marmara, Black, Azov and Caspian Seas. Marine Micropaleontology, 134, 1-152.

Naughton, F., Bourillet, J. F., Sánchez Goñi, M. F., Turon J. L., Jouanneau, J. M., 2007. Long-term and millennial-scale climate variability in northwestern France during the last 8850 years. The Holocene, 17(7), 939-953.

Penaud, A., Eynaud, F., Voelker, A. H. L., Turon J. L., 2016. Palaeohydrological changes over the last 50 ky in the central Gulf of Cadiz: complex forcing mechanisms mixing multi-scale processes. Biogeosciences, 13(18), 5357-5377.

Penaud, A., Ganne, A., Eynaud, F., Lambert, C., Coste, P. O., Herlédan, M., Vidal, M., Goslin, J., Stéphan, P., Charria, G., Pailler, Y., Durand, M., Zumaque, J., Mojtahid, M., 2020. Oceanic versus continental influences over the last 7 kyrs from a mid-shelf record in the northern Bay of Biscay (NE Atlantic). Quaternary Science Reviews, 229, 106135.

Pospelova, V., Kim, S. J., 2010. Dinoflagellate cysts in recent estuarine sediments from aquaculture sites of southern South Korea. Marine Micropaleontology, 76(1-2), 37-51.

Price, A. M., Coffin, M. R., Pospelova, V., Latimer, J. S., Chmura, G. L., 2017. Effect of nutrient pollution on dinoflagellate cyst assemblages across estuaries of the NW Atlantic. Marine pollution bulletin, 121(1-2), 339-351.

Price, A. M., Baustian, M. M., Turner, R. E., Rabalais, N. N., Chmura, G. L., 2018. Dinoflagellate cysts track eutrophication in the Northern Gulf of Mexico. Estuaries and Coasts, 41(5), 1322-1336.

Radi, T., de Vernal, A., 2004. Dinocyst distribution in surface sediments from the northeastern Pacific margin (40–60 N) in relation to hydrographic conditions, productivity and upwelling. Review of Palaeobotany and Palynology, 128(1-2), 169-193.

Reid, P. C., 1972. Dinoflagellate cyst distribution around the British Isles. Journal of the Marine Biological Association of the United Kingdom, 52(4), 939-944.

Reid, P. C., 1975. A regional sub-division of dinoflagellate cysts around the British Isles. New Phytologist, 75(3), 589-603.

Rochon, A., Vernal, A. D., Turon, J. L., Matthiessen, J., Head, M. J., 1999. Distribution of recent dinoflagellate cysts in surface sediments from the North Atlantic Ocean and adjacent seas in relation to sea-surface parameters. American Association of Stratigraphic Palynologists Contribution Series, 35, 1-146.

Sangiorgi, F., Donders, T. H., 2004. Reconstructing 150 years of eutrophication in the north-western Adriatic Sea (Italy) using dinoflagellate cysts, pollen and spores. Estuarine, Coastal and Shelf Science, 60(1), 69-79.

Stanisière J. Y., Mazurié J., Bouget J. F., Langlade A., Gabellec R., Retho M., Quinsat K., Leclerc E., Cugier P., Dussauze M., Menesguen A., Dumas F., Gohin F., Augustin J. M., Ehrhold A., Sinquin J. M., Goubert E., Dreano A., 2013. *Les risques conchylicoles en Baie de*

Quiberon. Troisième partie : le risque d'hypoxie pour l'huître creuse <u>Crassostrea gigas</u>. Rapport final du projet Risco 2010-2013. RST/LER/MPL/13.21.

Stockmarr, J. A., 1971. Tabletes with spores used in absolute pollen analysis. Pollen spores, 13, 615-621.

Taylor F. J. R., 1987. *The Biology of Dinoflagellates*. Blackwell Scientific, Oxford, 785 pp.

Tessier, C., 2006. *Caractérisation et dynamique des turbidités en zone côtière : l'exemple de la région marine Bretagne Sud*. Doctoral dissertation, University of Bordeaux, France, 428 pp.

Vanney, J. R., 1965. Étude sédimentologique du Mor Bras, Bretagne. Marine Geology, 3(3), 195-222.

Van Nieuwenhove, N., Head, M. J., Limoges, A., Pospelova, V., Mertens, K. N., Matthiessen, J., De Schepper, S., de Vernal, A., Eynaud, F., Londeix, L., Marret, F., Penaud, A., Radi, T., Rochon, A., 2020. An overview and brief description of common marine organic-walled dinoflagellate cyst taxa occurring in surface sediments of the Northern Hemisphere. Marine Micropaleontology, 159, 101814.

Von Stosch, H. A., 1973. Observations on vegetative reproduction and sexual life cycles of two freshwater dinoflagellates, *Gymnodinium pseudopalustre* Schiller and *Woloszynskia apiculate* sp. nov. British Phycological Journal, 8,105–134.

Wall, D., Dale, B., Lohman, G.P., Smith, W.K., 1977. The environmental and climatic distribution of dinoflagellate cysts in the North and South Atlantic Oceans and adjacent seas. Marine Micropaleontology. 2, 121-20.

Williams, D. B., 1971. The distribution of marine dinoflagellates in relation to physical and chemical conditions. In The micropalaeontology of oceans (pp. 91-95). Cambridge University Press Cambridge.

Zonneveld, K. A., Versteegh, G. J., de Lange, G. J., 1997. Preservation of organic-walled dinoflagellate cysts in different oxygen regimes: a 10,000-year natural experiment. Marine micropaleontology, 29(3-4), 393-405.

Zonneveld, K. A., Versteegh, G. J., de Lange, G. J., 2001. Palaeoproductivity and post-depositional aerobic organic matter decay reflected by dinoflagellate cyst assemblages of the Eastern Mediterranean S1 sapropel. Marine Geology, 172(3-4), 181-195.

Zonneveld, K. A., Bockelmann, F., Holzwarth, U. 2007. Selective preservation of organic-walled dinoflagellate cysts as a tool to quantify past net primary production and bottom water oxygen concentrations. Marine Geology, 237(3-4), 109-126.

Zonneveld, K. A., Versteegh G., Kodrans-Nsiah, M., 2008. Preservation and organic chemistry of Late Cenozoic organic-walled dinoflagellate cysts: A review. Marine Micropaleontology, 68(1-2), 179-197.

Zonneveld, K. A., Marret, F., Versteegh, G. J., Bogus, K., Bonnet, S., Bouimetarhan, I., Crouch, E., de Vernal, A., Elshanawany, A., Edwards, L., Esper, O., Forke, S., Grøsfjeld, K., Henry, M., Holzwarth, U., Kielt, J. F., Kim, S. Y., Ladouceur, S., Ledu, D., Chen, L., Limoges, A., Londeix, L., Lu, S. H., Mahmoud, M. S., Marino, G., Matsuoka, K., Matthiessen, J., Mildenhal, D. C., Mudie, P., Neil, H. L., Pospelova, V., Qi, Y., Radi, T., Richerol, T., Rochon, A., Sangiorgi, F., Solignac, S., Turon, J. L., Verleye, T., Wang, Y.,

Wang, Z., Young, M., 2013. Atlas of modern dinoflagellate cyst distribution based on 2405 data points. Review of Palaeobotany and Palynology, 191, 1-197.

Zonneveld, K. A., Pospelova, V., 2015. A determination key for modern dinoflagellate cysts. Palynology, 39(3), 387-409.

Zumaque, J., Eynaud, F., de Vernal, A., 2017. Holocene paleoceanography of the Bay of Biscay: evidence for West-East linkages in the North Atlantic based on dinocyst data. Palaeogeography, Palaeoclimatology, Palaeoecology, 468, 405-413.

Figures
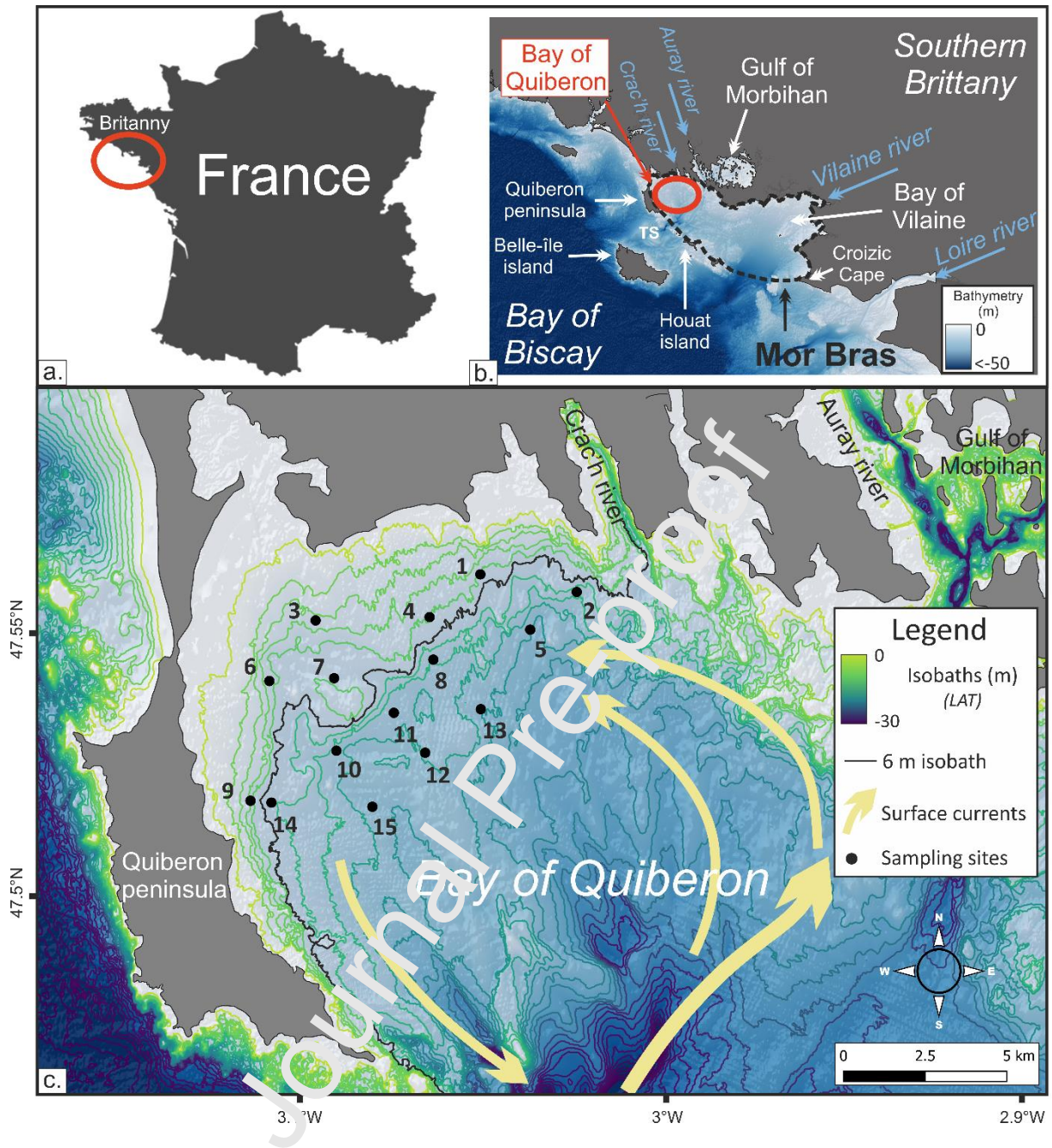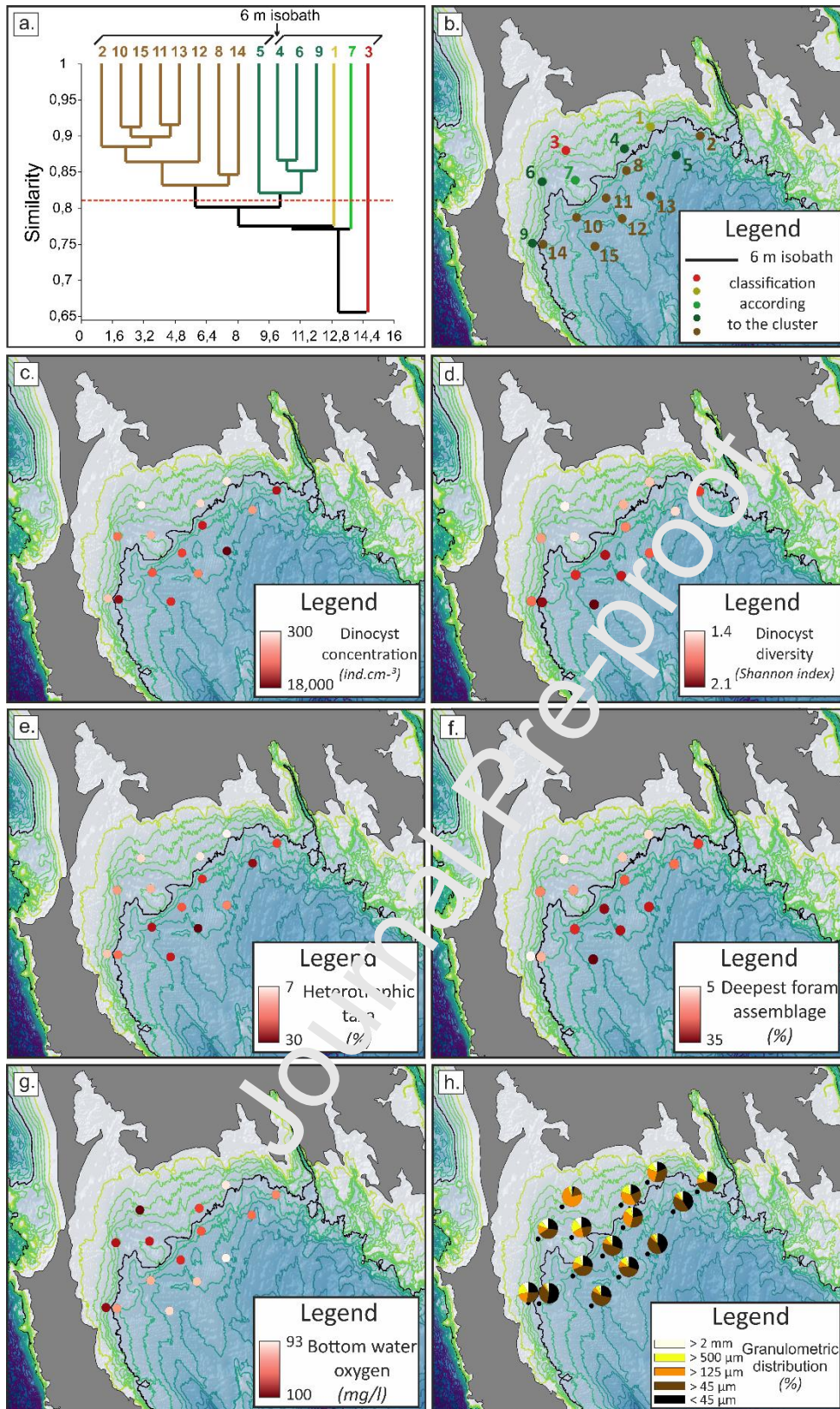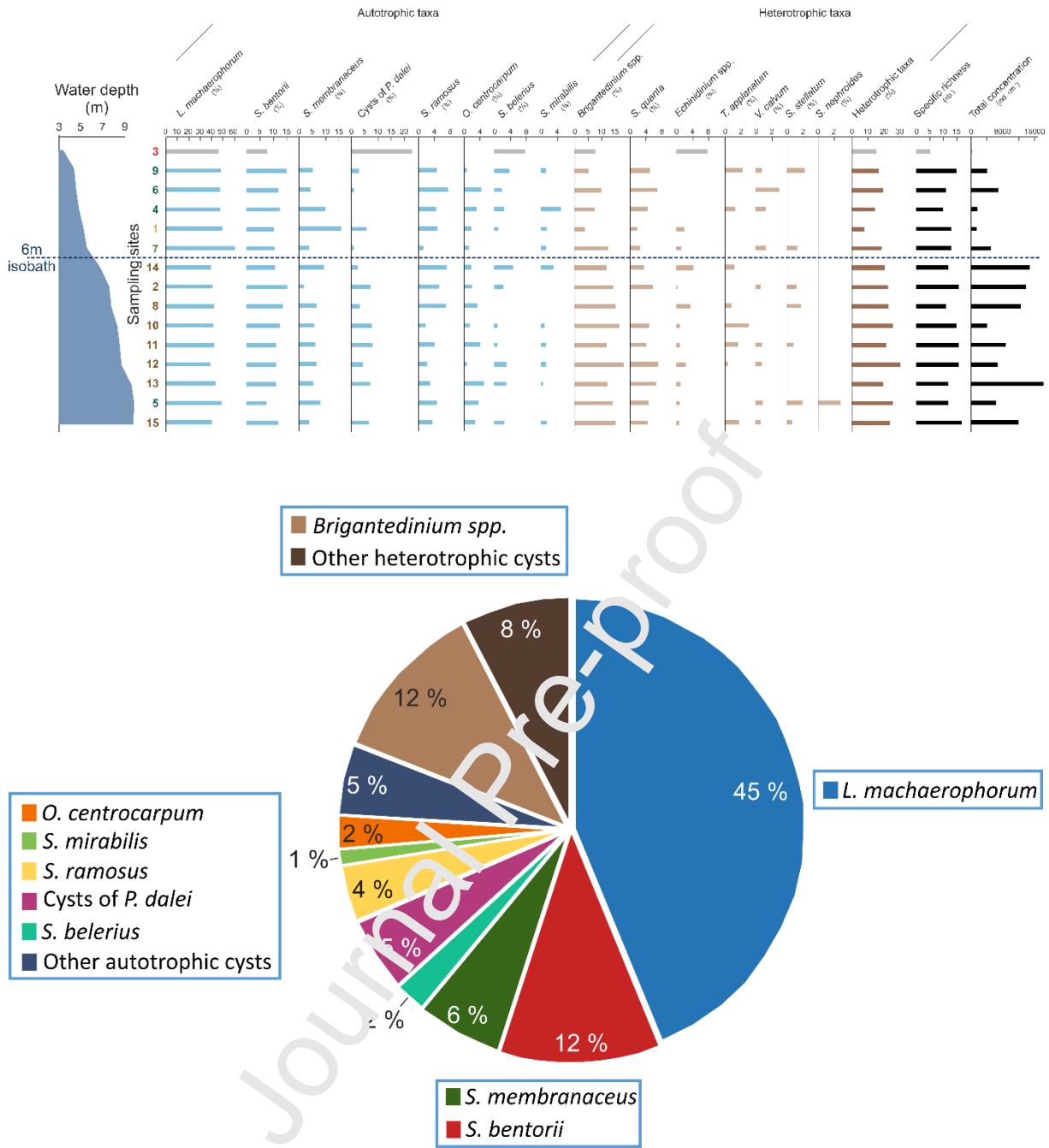
Figure 1

Figure 2

Figure 3

	Hdino	Srdino	Cdino	depth	Temp	Sal	O2	Chla	Turb	SM	granulo <125	Deep Foram
Hdino		0.106	0.072	0.003	0.245	0.067	0.369	0.846	0.567	0.574	0.029	0.001
Srdino	0.43		0.182	0.028	0.004	0.293	0.025	0.812	0.096	0.897	0.017	0.062
Cdino	0.48	0.63		0.006	0.099	0.175	0.028	0.764	0.046	0.871	0.001	0.028
depth	0.71	0.61	0.67		0.000	0.187	0.004	0.734	0.204	0.977	0.000	0.000
Temp	-0.32	-0.65	-0.44	-0.79		0.576	0.001	0.761	0.038	0.616	0.012	0.003
Sal	0.48	0.43	0.37	0.36	-0.16		0.932	0.536	0.013	0.058	0.093	0.270
O2	-0.25	-0.59	-0.56	-0.70	0.76	-0.02		0.702	0.145	0.783	0.002	0.030
Chla	-0.06	0.13	-0.09	-0.10	0.09	-0.17	0.11		0.347	0.183	0.385	0.908
Turb	0.16	0.55	0.52	0.35	-0.54	0.63	-0.40	-0.26		0.729	0.053	0.383
SM	-0.16	-0.14	0.05	-0.01	-0.14	-0.50	-0.08	-0.36	-0.10		0.871	0.705
granulo <125	0.56	0.77	0.75	0.80	-0.63	0.45	-0.73	-0.25	0.51	-0.05		0.004
Deep Foram	0.65	0.66	0.51	0.80	-0.70	0.49	-0.52	0.16	0.40	-0.18	0.62	

p-value

correlation coefficient (r)
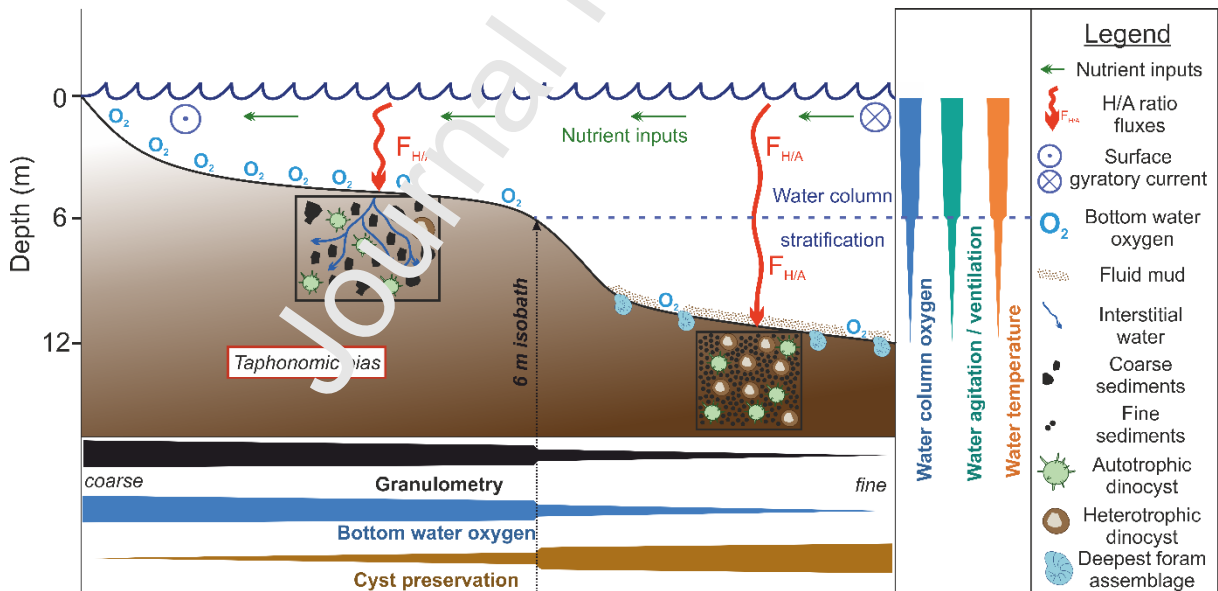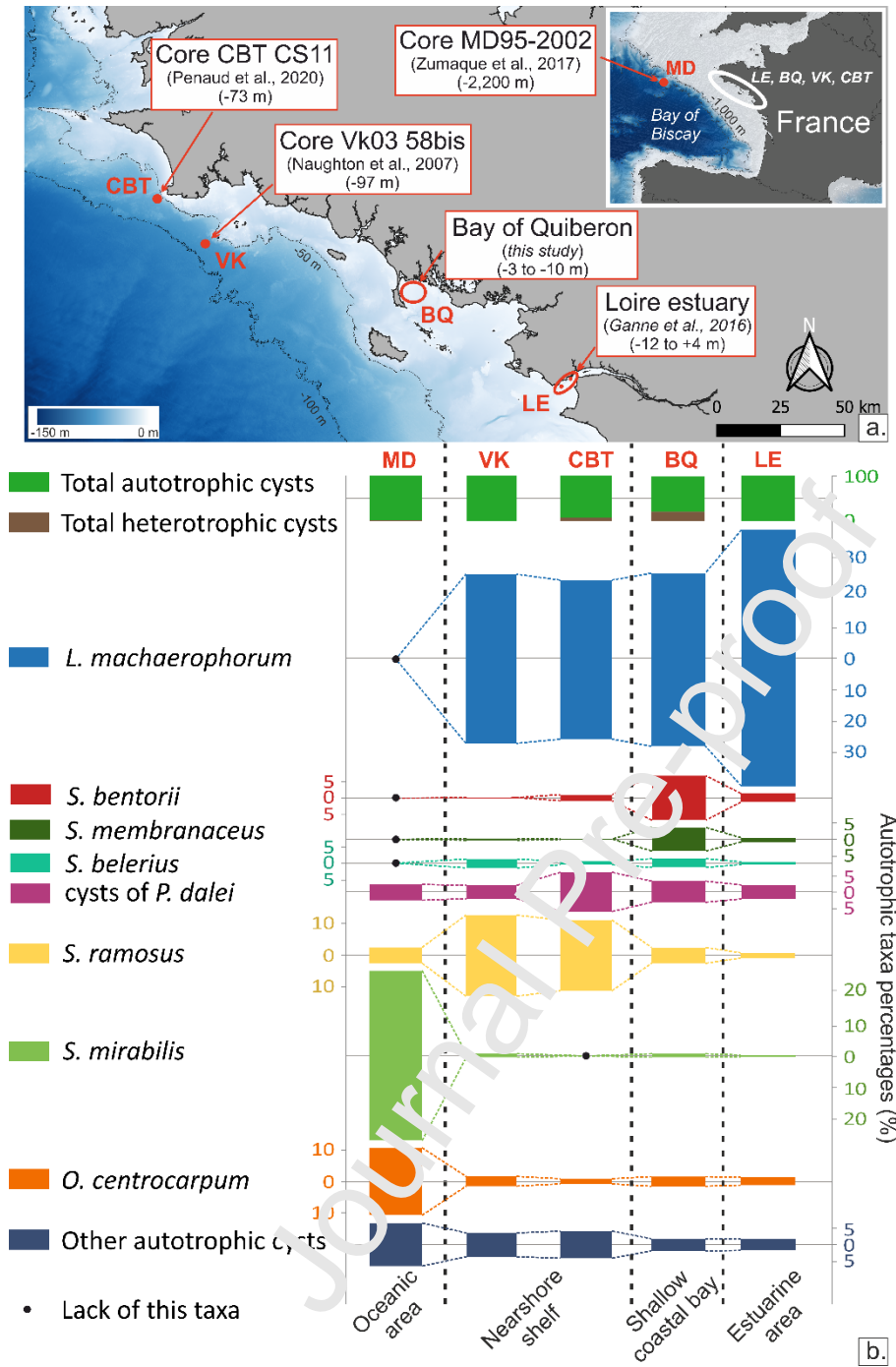
Figure 4

Figure 5:

Figure 6

Site	Longitude	Latitude	Sampling depth (m)
1	-3.0501	47.5592979	5.24
2	-3.02359375	47.5560063	7.57

3	-3.09542143	47.5507071	3.37
4	-3.06407917	47.5513313	4.82
5	-3.03639167	47.5489833	9.83
6	-3.10814524	47.5394214	4.58
7	-3.09032917	47.5399396	5.55
8	-3.0630375	47.5434083	7.77
9	-3.11331927	47.5170971	4.4
10	-3.08969323	47.5264333	8.3
11	-3.0739	47.5334896	8.52
12	-3.06528125	47.52605	8.69
13	-3.04997917	47.5341708	9.6
14	-3.10756875	47.5167321	6.75
15	-3.07979245	47.5150747	9.74

Table 1

Site	depth (m)	Srdino	Cdino (nb./cm³)	Hdino (%)	Temp (°C)	Sal (‰)	O2 (mg/l)	Chla (µg/l)	Turb (NTU)	SM (mg/l)	DeepForam (%)	granulo< 125 (%)
1	5.24	1.78	1504.49	7.6	14.5	34.3	93.55	1.95	2.04	6.23	6	54
2	7.57	1.94	13979.95	22.7	14.5	34.4	94.77	1.56	2.40	7.06	12	72
3	3.37	1.48	332.14	15.4	14.8	34.5	100.53	1.94	1.77	5.34	5	21

4	4.82	1.78	1704.96	14.6	14.6	34.4	95.56	1.94	2.09	4.16	8	42
5	9.83	1.77	6313.97	25.9	14.5	34.5	94.84	1.48	1.97	5.29	17	84
6	4.58	1.84	6949.33	19.4	14.7	34.5	96.31	1.89	2.30	4.51	8	66
7	5.55	1.53	5066.16	18.2	14.7	34.5	96.09	1.76	2.03	4.62	10	47
8	7.77	1.87	12657.71	22.7	14.6	34.4	95.25	2.23	1.81	5.17	14	54
9	4.4	1.93	4067.19	16.5	14.6	34.6	97.84	1.81	2.80	4.68	6	52
10	8.3	1.96	8749.84	25.3	14.5	34.5	94.58	2.11	2.17	4.02	14	67
11	8.52	2.03	8831.44	21.2	14.5	34.5	96.02	2.22	2.06	4.63	17	78
12	8.69	2.02	6781.88	30.0	14.5	34.6	94.50	2.00	2.55	5.05	16	74
13	9.6	1.94	18287.72	19.5	14.4	34.6	93.23	1.83	3.30	4.90	17	87
14	6.75	2.03	14767.33	20.6	14.7	34.6	94.67	1.83	2.28	4.51	9	89
15	9.74	2.10	12019.51	23.3	14.4	34.7	93.61	1.76	2.74	4.48	15.08	82

Table 2

Abbreviation	Cyst-based taxonomy	Motile stage-based taxonomy	Autotrophic or Heterotrophic	Mean %
ACHO	*Ataxodinium choane*	*Gonyaulax spp.* ?	A	0.3
ISPH	*Impagidinium sphaericum*	*Gonyaulax spp.* ?	A	< 0.1
LMAC	*Lingulodinium machaerophorum*	*Lingulodinium polyedra*	A	45.3
OCEN	*Operculodinium centrocarpum*	*Protoceratium reticulatum*	A	2.5
OISR	*Operculodinium israelianum*	*Protoceratium spp.* ?	A	< 0.1
PDAL	Cyst of *Pentapharsodinium dalei*	*Pentapharsodinium dalei*	A	5.4
SBEL	*Spiniferites belerius*	Unknown	A	2.3
SBEN	*Spiniferites bentorii*	*Gonyaulax digitale* ?	A	11.5
SDEL	*Spiniferites delicatus*	*Gonyaulax spp.* ?	A	0.6
SMEM	*Spiniferites membranaceus*	*Gonyaulax spp.* (*membranacea* ?)	A	6.3
SMIR	*Spiniferites mirabilis*	*Gonyaulax spinifera* ?	A	1.1
SRAM	*Spiniferites ramosus*	*Gonyaulax spp.* ?	A	4.1
BSPP	*Brigantedinium spp.*	*Protoperidinium spp.* ?	H	11.8
ESPP	*Echinidinium spp.*	*Protoperidinium spp.* ?	H	1.7
GCAT	Cyst of *Gymnodinium catenatum*	*Gymnodinium catenatum*	H	0.1
GSPP	Cyst of *Gymnodinium spp.*	*Gymnodinium spp.*	H	< 0.1
LSAB	*Lejeunecysta sabrina*	*Protoperidinium leonis* ?	H	0.1
PAME	Cyst of *Protoperidinium americanum*	*Protoperidinium americanum*	H	0.1
PSPP	Cyst of *Protoperidinium spp.*	*Protoperidinium spp.*	H	< 0.1
SNEP	*Selenopemphix nephroides*	*Protoperidinium*	H	0.2

		subinerme		
SQUA	*Selenopemphix quanta*	*Protoperidinium conicum*	H	4.2
STEL	*Stelladinium stellatum*	*Protoperidinium compressum*	H	0.6
TAPP	*Trinovantedinium applanatum*	*Protoperidinium pentagonum*	H	0.8
VCAL	*Votadinium calvum*	*Protoperidinium oblongum ?*	H	0.7
VSPI	*Votadinium spinosum*	*Protoperidinium claudicans*	H	< 0.1
XAND	*Xandarodinium xanthum*	*Protoperidinium divaricatum*	H	0.1

Table 3

Figure captions:

Figure 1: a) Location of the study area in NW France. b) Zoom on the S Brittany area identified in a): main bays and rivers are highlighted in the map, as well as the investigated Bay of Quiberon (BQ). The 'Mor Bras' is a bathymetric depression bordering the southern coast of Brittany. c) Distribution of the 15 sampling sites within the BQ. The yellow arrows represent the residual gyratory tidal currents (*Vanney, 1965; Lemoine, 1989; Tessier, 2006*). Maps are performed using the SHOM bathymetric data (SHOM, 2015. '*MNT Bathymétrique de façade Atlantique*' (Homonim Project).

http://dx.doi.org/10.17183/MNT_ATL100m_HOMONIM_WGS84). LAT = "Lowest Astronomical Tides", chart datum.

Figure 2: Distribution maps of various palynological and environmental parameters within the BQ. a) Clustering of sampling stations according to the relative abundances of dinocyst taxa (using PAST v.1.75b; Hammer et al., 2001); b) Colorization of sampling stations according to their membership group in the cluster; c) Dinocyst concentrations (number of specimens/cm^3); d) Dinocyst diversity (Shannon diversity index); e) Heteretrophic dinocyst taxa percentages; f) Proportion of the 'deep foraminiferal assemblage' regarding the total benthic foraminifera taxa (as described in section 2.); g) Bottom water oxygen concentrations; h) Percentages of grain-size classes.

Figure 3: a) Diagram representing the percentages of the main dinocyst taxa (greater than 2% on at least one study site), as well as the number of taxa and the total dinocyst concentration, for each BQ study sample. Sampling sites are classified according to water depth. Sample n°3 (with only 13 individuals counted) is highlighted in grey. The station numbers (to the left of the diagram) are highlighted with the colors identified in the cluster (Fig. 2). b) Averaged percentages of the dominant dinocyst taxa recorded in the fifteen BQ samples.

Figure 4: Correlation matrix of the different environmental, foraminiferal and dinocyst taxa presented in Tables 2 and 3. A color gradient from blue to red is used to represent the correlation coefficients (blue is used for negative values and red for positive ones; the higher the absolute value (i.e. when it tends to 1), the darker the color). Regarding the other half of the matrix, only p-values below 0.1 are highlighted in light (0.1<p-value<0.01) and dark (p-value<0.1) green.

Figure 5: Conceptual model presenting the taphonomic preservation bias impacting dinocysts (especially heterotrophics and dinocyst concentrations) in the shallow Bay of Quiberon, on

either side of the 6 m bathymetric threshold. The red arrows represent dinocyst fluxes to the sediments. H/A: ratio Heterotrophic to Autotrophic dinocysts. Due to homogenized hydrological parameters of the surface waters within the BQ, we consider that the H/A ratio and nutrient concentrations remain stable at the BQ scale. Gradients for particle size, oxygen concentration, and dinocyst preservation are highlighted under the figure with horizontal thicker or thinner lines on either side of the 6m isobath, and gradients for oxygen concentration, sea-surface temperature and water column mixing are highlighted to the right of the figure with vertical thicker or thinner lines according to the BQ water depth.

Figure 6: a) Location of modern samples and core tops used in the inshore-offshore transect at the southern Brittany-scale. Map performed using the SHOM bathymetric data (SHOM, 2015. '*MNT Bathymétrique de façade Atlantique*' (Homonim Project). http://dx.doi.org/10.17183/MNT_ATL100m_HOMONIM_WGS84) and depths are given according to the chart datum. b) Selected dinocyst taxa percentages: heterotrophics vs. autotrophics for the first line and percentages of the major taxa based on a main autotrophic sum (i.e. excluding heterotrophics). Sites are presented, from right to left, according to their distance from continental influences: LE for 'Loire estuary', BQ for 'Bay of Quiberon', CBT for 'Core CBT-CS11', VK for 'Core VK03-58bis' and MD for 'Core MD95-2002').

Table 1: Geographic coordinates of sampling sites. Sampling depths ('depth' in the correlation matrix of variables) are provided according to the chart datum ('lowest astronomical tides').

Table 2: Values of the environmental quantitative parameters used in the correlation matrix of variables for each sampling station (cf. Fig. 4).

Table 3: List of dinocyst taxa (and their thecate name) identified in this study, abbreviations and percentages recorded in the averaged fifteen BQ surface sediment samples.

Declaration of interests

☒ The authors declare that they have no known competing financial interests or personal relationships that could have appeared to influence the work reported in this paper.

☐The authors declare the following financial interests/personal relationships which may be considered as potential competing interests:

1. Dinocyst distribution in a French coastal bay linked to environmental parameters.
2. Proportions of heterotrophic dinocysts related to oxidation processes.
3. Lower dinocyst diversity observed under "higher O_2-coarser sediments".
4. Dinocyst distribution along a northern Bay of Biscay inshore-offshore gradient.